PHYSICAL REVIEW B **79**, 075442 (2009)

Parametric interatomic potential for graphene

V. K. Tewary*
Materials Reliability Division, National Institute of Standards and Technology, Boulder, Colorado 80305, USA

B. Yang
Department of Mechanical and Aerospace Engineering, Florida Institute of Technology, Melbourne, Florida 32901, USA

(Received 14 November 2008; published 27 February 2009)

A parametric interatomic potential is constructed for graphene. The potential energy consists of two parts: a bond energy function and a radial interaction energy function. The bond energy function is based on the Tersoff-Brenner potential model. It includes angular terms and explicitly accounts for flexural deformation of the lattice normal to the plane of graphene. It determines the cohesive energy of graphene and its equilibrium lattice constant. The radial energy function has been chosen such that it does not contribute to the binding energy or the equilibrium lattice constant but contributes to the interatomic force constants. The range of interaction of each atom extends up to its fourth-neighbor atoms in contrast to the Tersoff-Brenner potential, which extends only up to second neighbors. The parameters of the potential are obtained by fitting the calculated values to the cohesive energy, lattice constant, elastic constants, and phonon frequencies of graphene. The values of the force constants between an atom and other atoms that are within its fourth-neighbor distance are calculated. Analytical expressions are given for the elastic constants and the flexural rigidity of graphene. The flexural rigidity of the graphene lattice is found to be 2.13 eV, which is much higher than 0.797 eV calculated earlier using the Tersoff-Brenner potential.

DOI: 10.1103/PhysRevB.79.075442 PACS number(s): 61.48.De, 81.05.Uw, 63.20.D−, 63.22.−m

I. INTRODUCTION

We construct a parametric interatomic potential for graphene that reproduces its cohesive energy, lattice constant, elastic constants, and phonon spectra. We use the potential to calculate the flexural rigidity of graphene. These characteristics determine the thermomechanical stability and reliability of a material, which must be studied for its industrial applications. Knowledge of the interatomic potential is also necessary for computer simulation of the structural properties of materials. A large amount of work has been done on the electronic characteristics of graphene but relatively less work has been reported on modeling its thermal and mechanical characteristics. Our interest in this paper is only in the mechanical characteristics of graphene and not in its electronic characteristics.

Although the discovery of graphene is new, it has been theoretically studied for a long time as a building block of oriented graphite. An oriented graphite crystal such as highly oriented pyrolitic graphite can be visualized as a set of weakly bound graphene sheets for estimating its mechanical characteristics though not electronic characteristics. Since the binding between atoms in different planes is much weaker than those in the same plane, many experimental observations in graphite can be applicable to graphene. This applies to the observed phonon spectra of graphite which can be assumed to approximately represent the phonon spectra of graphene except at very low frequencies. Similarly the elastic constants $c11$ and $c66$ of graphite with reference to its crystallographic axes can be regarded as approximately the elastic constants of graphene. This correspondence is useful for modeling the mechanical characteristics of graphene since it is not easy to measure mechanical properties of single sheets of graphene.

Methods for calculating the interatomic potential of graphene can be classified within two broad categories: *ab initio* and parametric. For a review and other references, please see the excellent article by Qian *et al.*[1] The *ab initio* methods (see, for example, Refs. 2–7) are computationally extensive and expected to be more reliable. However, in practice, they sometimes make simplifying assumptions of questionable validity. The parametric or empirical methods consist of assuming a functional form for the potential and fitting the parameters of the function with the experimental results. One advantage of the parametric methods is that they give the potential for a material in an analytical form, which is convenient for subsequent calculations of other properties of the material. Our interest in this paper is only in the parametric potentials.

Several parametric and bond-order potentials[1,8–13] have been proposed for carbon atoms in nanotubes, graphene or graphite, and other solids. An excellent bond-order potential for graphite has recently been constructed by Los *et al.*[14] It is a very detailed potential that accounts for the coordination number, various correlations, and distortion effects and is applicable to study of phase change. These details inevitably make the form of the potential rather complicated. This complexity may not be needed for many simpler applications such as static calculations and phonon spectra that depend on mainly the force constants and the potential near the lattice sites. It has not yet been applied to calculate the force constants and phonon spectrum of graphite or graphene.

A popular choice for the interatomic potential seems to be the Tersoff-Brenner (TB) potential.[8,11] It accounts for the angular forces and gives the correct cohesive energy and the equilibrium lattice constant of graphene. It is very general and applicable to a wide range of configurations. However, it does not correctly reproduce the elastic constants of

graphene and the phonon-dispersion curves possibly because the range of interatomic interactions in the TB potential is limited to only up to second neighbors of each atom. The short-range nature of the potential is unrealistic for modeling phonons in graphene. It is known that interactions up to at least fourth neighbors[6] or even fifth neighbors[15] must be included in the interatomic potential in order to reproduce the phonon frequencies for graphene.

The TB potential has the great advantage of simplicity for lattice statics and simulation calculations. It seems to be worthwhile, therefore, to generalize the TB model, without sacrificing its inherent simplicity, so that it is also applicable to lattice statics and lattice dynamics calculations. In this paper, we present a functional form of the interatomic potential for graphene which is partly based on the TB model potential. We write the total potential energy of an atom as a sum of two parts: a bond energy part and a radial interaction part. The bond energy function has the same form as in the TB potential. We keep the same exponential terms but modify the coefficients that represent angular forces. This part correctly gives the cohesive energy and the equilibrium lattice constant of graphene. In this part, we explicitly introduce the dependence of the potential on the Z components of the atomic displacements, where the graphene plane is assumed to be in the XY plane and the Z axis is normal to the graphene plane. It is particularly important to model the out-of-plane displacements explicitly in view of the recent observations of ripples in graphene.[16] The XY component of the bond potential extends up to second neighbors of each atom as in the TB potential, but the Z component extends up to fourth neighbors.

The radial part of our potential extends up to fourth-neighbor atoms. The radial function has been chosen such that it does not contribute to the cohesive energy and the equilibrium lattice constant of graphene but contributes to the interatomic force constants. The parameters of the potential function are obtained by fitting with the observed cohesive energy, equilibrium lattice constant, elastic constants, and the phonon frequencies in the ΓM, ΓK, and MK directions. The phonon frequencies are calculated in terms of the interatomic force constants, which are calculated from the potential and extend up to fourth nearest neighbors of each atom.

We derive analytical expressions for the elastic constants and the flexural rigidity of graphene in terms of the force constants. For the elastic constants, we use the method of long waves,[17] and for the flexural rigidity we use the formula obtained by Green's-function method.[18] We obtain a flexural rigidity of 2.13 eV in contrast to 0.797 eV obtained by using the TB potential, as reported earlier.[18] Since the force constants derived in the present paper give a better fit with the experimentally observed phonon dispersion, the present value of the flexural rigidity should be more reliable.

The potential is described in Sec. II. The values of the interatomic force constants, the phonon spectra, the elastic constants, and the flexural rigidity of graphene are calculated in Sec. III. A brief discussion of the results and conclusions are presented in Sec. IV.

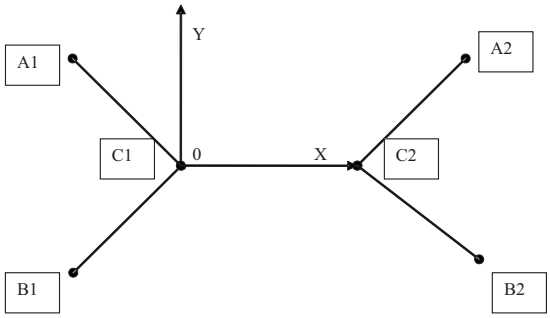

FIG. 1. The bond structure of hexagonal graphene and the coordinate axes. The dots show the lattice sites occupied by carbon atoms A1, B1, C1, A2, B2, and C2. The origin of coordinates is at C1.

II. FUNCTIONAL FORM OF THE POTENTIAL

We write the potential energy W of an atom, called the reference atom, as a sum of two parts as given below,

$$W = W_b + W_r, \tag{1}$$

where W_b is the bond energy per atom and W_r is the radial interaction energy of each atom. The radial part extends up to fourth-neighbor atoms of the reference atom and will be defined later. The bond energy W_b is the energy of the bond per atom connecting the reference atom to its nearest neighbors. It includes the angular forces and depends on the location of other atoms. Consider the bond between atoms C1 and C2 in a graphene lattice as shown in Fig. 1. Atoms A1 and B1 are the two other nearest neighbors of C1. Similarly A2 and B2 are nearest neighbors of C2. As in the TB model, we write W_b as the following:

$$W_b = AF_{C1}F_{C2}\exp(-\alpha r) - B\exp(-\beta r), \tag{2}$$

where r is the distance between C1 and C2, α, β, A, and B are constants, and the functions F_{C1} and F_{C2} depend on the location of other neighbors of atoms C1 and C2. The first and the second terms on the right-hand side (RHS) of Eq. (2) represent the attractive and the repulsive parts of the Morse potential as used in the TB model.

The values of α and β are same as those given by Brenner.[8] The constants A and B are determined from the equilibrium value of the lattice constant and the condition that the total energy given by Eq. (1) at equilibrium is equal to the cohesive energy of graphene. However, the radial potential function W_r has been chosen such that it does not contribute to the total energy or its minimum for the graphene lattice at equilibrium, so A and B are determined from W_b alone.

The functions F_{C1} and F_{C2} contain parameters that we obtain by fitting to the experimental results. We could include functions similar to F_{C1} and F_{C2} in the second term in Eq. (2) as well, if needed for better fitting with the experimental results, but we did not find that to be necessary in the present work.

The functions F_{C1} and F_{C2} may be physically visualized as the effective charge densities on atoms C_1 and C_2, respectively. Each function contains a sum of contributions from

the nearby atoms. We can introduce separate envelope functions around C1 and C2, which define the region of influence (ROI) for C1 and separately for C2. The atoms in the ROI of C1 will contribute to F_{C1} and similarly for F_{C2}. For out-of-plane deformations, we will also include some cross terms in which the atoms in the ROI of C1 will contribute to F_{C2} and vice versa. As in the TB model, the envelope functions are not optimized. They serve the purpose only of restricting the range of the ROI and, thus, help identify the atoms that contribute to F_{C1} and F_{C2}. The actual mathematical form of the envelope function does not affect our calculations. We can therefore assume the same envelope functions as in the TB model.[8,11] In the present case, the ROIs of atoms C1 and C2 are restricted to only their nearest neighbors. In Fig. 1, the ROI of C1 contains atoms A1 and B1and the ROI of C2 contains atoms A2 and B2. Obviously C1 and C2 themselves are not included in the ROI since we are calculating the energy of the bond C1C2.

We first consider F_{C1}. It contains contributions of atoms A1 and B1. The contribution of each atom depends on the angle it forms with different bonds, its distance from atom C1, and its projection on the planes containing other atoms and the bond C1C2. We denote the length of the vector from C1 to A1 by $M(\mathrm{C1,A1})$ and the unit vector along the line from C1 to A by $\mathbf{V}(\mathrm{C1,A1})$. The cosine square of the angle between two vectors such as $\mathbf{V}(\mathrm{C1,A1})$ and $\mathbf{V}(\mathrm{C1,B1})$ is given by

$$\theta(\mathrm{A1,C1,B1}) = [\mathbf{V}(\mathrm{C1,B1}) \cdot \mathbf{V}(\mathrm{C1,A1})]^2, \tag{3}$$

where the dot between the two vectors denotes their dot product. We further define unit vectors N normal to the plane of three atoms, A1, C1, and C2, as follows:

$$\mathbf{N}(\mathrm{A1,C1,C2}) = \mathbf{V}(\mathrm{C1,A1}) \times \mathbf{V}(\mathrm{C1,C2})/|\mathbf{V}(\mathrm{C1,A1}) \times \mathbf{V}(\mathrm{C1,C2})|, \tag{4}$$

where $\times$ denotes the cross product and the vertical lines denote the magnitude of the enclosed vector. In case of a perfectly planar graphene lattice all the N vectors are normal to the plane of the lattice and $\theta(\mathrm{A1,C1,B1}) = \cos^2(2\pi/3) = 1/4$ at equilibrium.

We write F_{C1} as a sum of the contributions $f_{A1,C1}$ and $f_{B1,C1}$ from A1 and B1, respectively, as follows:

$$F_{C1} = f_{A1,C1} + f_{B1,C1}, \tag{5}$$

where

$$f_{A1,C1} = \exp[-D(\mathrm{A1,C1}) - E(\mathrm{A1,C1})], \tag{6}$$

$$D(\mathrm{A1,C1}) = \mu_1 P(\mathrm{A1,C1,C2}) + \mu_2 P(\mathrm{A1,C1,B1}) + \gamma[M(\mathrm{C1,A1}) - a_0], \tag{7}$$

$$E(\mathrm{A1,C1}) = \lambda_1 U(\mathrm{A1,C1}) + \lambda_2 T(\mathrm{A1,C1}), \tag{8}$$

$$P(\mathrm{A1,C1,C2}) = \theta(\mathrm{A1,C1,C2}) - \cos^2 2\pi/3, \tag{9}$$

$$P(\mathrm{A1,C1,B1}) = \theta(\mathrm{A1,C1,B1}) - \cos^2 2\pi/3, \tag{10}$$

$$U(\mathrm{A1,C1}) = [\mathbf{V}(\mathrm{C1,A1}) \cdot \mathbf{N}(\mathrm{A1,C1,C2})]^2 + [\mathbf{V}(\mathrm{C1,A1}) \cdot \mathbf{N}(\mathrm{B1,C1,C2})]^2 + [\mathbf{V}(\mathrm{C1,A1}) \cdot \mathbf{N}(\mathrm{A2,C1,C2})]^2 + [\mathbf{V}(\mathrm{C1,A1}) \cdot \mathbf{N}(\mathrm{B2,C1,C2})]^2, \tag{11}$$

$$T(\mathrm{A1,C1}) = [\mathbf{N}(\mathrm{A1,C1,B1}) \cdot \mathbf{N}(\mathrm{A2,C2,C1})]^2 + [\mathbf{N}(\mathrm{A1,C1,B1}) \cdot \mathbf{N}(\mathrm{B2,C2,C1})]^2, \tag{12}$$

where a_0 is a constant equal to the length of the undistorted graphene bond and μ_i, λ_i, and γ are adjustable parameters, which we determine by fitting the calculated phonon-dispersion curves and the elastic constants with their experimental values. The first term on the RHS of Eq. (11) is obviously zero but is included so that the equation reflects the system of enumerating various contributions. For a perfect graphene lattice in equilibrium, $a_0 = M(\mathrm{C1,A1})$.

The function $f_{B1,C1}$ in Eq. (5) can be obtained from the above equations by interchanging A1 and B1. Similarly we define the charge density for atom C2 as

$$F_{C2} = f_{A2,C2} + f_{B2,C2}. \tag{13}$$

The form of the function $f_{A2,C2}$ can be written from Eqs. (6)–(12) by interchanging A1, B1, and C1 with A2, B2, and C2, respectively. Finally, $f_{B2,C2}$ is obtained from the expression for $f_{A2,C2}$ by interchanging A2 and B2. The above equations have been written for two atoms in each ROI. If there are more atoms in the ROI, their contributions can be included following the same system as used in the above equations.

We can now write the above equations in a general form that is more convenient for simulation calculations and is applicable to those cases in which an ROI may have more than two atoms, as in the case of clusters around graphene lattice sites. The bond energy between atoms I and J that are nearest neighbors to each other and connected by a bond is written as follows:

$$W_{bI,J} = AF_I F_J \exp(-\alpha r_{I,J}) - B \exp(-\beta r_{I,J}), \tag{14}$$

where

$$F_I = \sum_K f_{K,I} \quad (K \neq J \neq I), \tag{15}$$

$$f_{K,I} = \exp[-D_{K,I} - E_{K,I}], \tag{16}$$

$$D_{K,I} = \mu_1 P_{K,I,J} + \mu_2 \sum_{K'} P_{K,I,K'} + \gamma[M_{I,K} - a_0] \quad (K' \neq K), \tag{17}$$

$$E_{K,I} = \lambda_1 U_{K,I} + \lambda_2 T_{K,I}, \tag{18}$$

$$P_{K,I,J} = \theta_{K,I,J} - \cos^2(2\pi/3), \tag{19}$$

$$P_{K,I,K'} = \theta_{K,I,K'} - \cos^2(2\pi/3) \quad (K' \neq K), \tag{20}$$

$$U_{I,K} = \sum_{K'} [V_{I,K} \cdot N_{K',I,J}]^2 + \sum_L [V_{I,K} \cdot N_{L,I,J}]^2, \tag{21}$$

$$T_{I,K} = \sum_{K'} \sum_{L} [N_{K,I,K'} \cdot N_{L,J,I}]^2. \quad (22)$$

In Eqs. (14)–(22), $r_{I,J}$ denotes the distance between atoms I and J, the indices K and K' label the atoms in the ROI of atom I, and L labels the atoms in the ROI of the atom J. The summation convention over repeated indices is not assumed.

We now consider the energy of a perfect graphene lattice as a function of the lattice constant as shown in Fig. 1. When all the atoms occupy the hexagonal sites, $D(\mathrm{A1,C1})$ and $E(\mathrm{A1,C1})$ in Eq. (6) are zero, $F_{\mathrm{C1}}=F_{\mathrm{C2}}=2$, and Eq. (2) reduces to the exponential Morse potential. Minimizing the energy of the perfect graphene lattice with respect to the lattice parameter or the nearest-neighbor distance and equating the minimum energy to the cohesive energy, we obtain at equilibrium

$$A = \frac{E_c \beta}{12(\beta - \alpha)} \exp(\alpha R_0) \quad (23)$$

and

$$B = \frac{E_c \alpha}{3(\beta - \alpha)} \exp(\beta R_0), \quad (24)$$

where R_0 is the equilibrium nearest-neighbor distance and E_c is the cohesive energy per atom. Since W_b is the bond energy per atom and $W_r=0$ at equilibrium, $E_c=3W_b$ corresponding to three bonds per atom.

For the radial energy part in Eq. (1) we choose the following polynomial function:

$$W_r = \exp[-\beta(r - R_4)] \sum_{i=1}^{4} v_i(r) m_i(r) \quad (r < R_e), \quad (25)$$

where

$$v_i(r) = Q_i(r - R_i) + S_i(r - R_i)^2, \quad (26)$$

$$m_i(r) = \prod_{j \neq i=1}^{4} (r - R_j)^3, \quad (27)$$

where Q_i and S_i are constants and R_i is the ith neighbor distance in the undeformed graphene lattice, and R_e is the range of the envelope function which restricts the range of the radial potential. At equilibrium $R_1=R_0$ which was defined in Eqs. (23) and (24). As in the TB model, we do not need to optimize the shape of the envelope function which may be taken as the step function being unity for $r<R_e$ and 0 for $r>R_e$. A convenient choice of R_e is slightly larger than the R_4 so that the range of interaction is limited to fourth neighbors of each atom and the parameters of the lattice are independent of R_e.

The form of W_r has been chosen such that it is zero at the hexagonal graphene lattice sites. Its contribution to the derivative with respect to the lattice parameter is also zero. Thus this function does not contribute to the cohesive energy or the value of the lattice constant which is determined from W_b. The first and second derivatives of W_r at the lattice sites are not zero. Thus W_r contributes to the interatomic force constants and hence to the phonon spectra. The values of the parameters in the potential function are given in Sec. III.

III. INTERATOMIC FORCE CONSTANTS AND THE PHONON SPECTRA

Unless stated otherwise, all lengths will be reported in units of a, where $2a=2.461$ Å is the lattice constant of graphene at equilibrium.[6] Our model potential has 13 adjustable parameters—5 in W_b and 8 in W_r. The 5 parameters in W_b are μ_1, μ_2, γ, λ_1, and λ_2. Out of these γ has the dimensions of inverse length and the remaining four are dimensionless. The 8 parameters in W_r are Q_i and S_i for $i=1-4$. All these have the dimensions of energy since r and R_i are expressed in units of a and are dimensionless. These 13 parameters are determined by fitting the calculated phonon frequencies and the two elastic constants $c11$ and $c66$ with the experimentally observed values, as will be described below. The constants α, β, A, B, and R_0 are not adjustable parameters. The values of the α and β are the same as those obtained by Brenner.[8] The constant R_0 in Eqs. (23) and (24) is equal to $2/\sqrt{3}$. For E_c we use the experimental value of 7.4 eV, as quoted by Brenner.[8] The constants A and B are then calculated from Eqs. (23) and (24).

In order to obtain the values of the 13 adjustable parameters, we calculate the phonon dispersion for graphene in symmetry directions ΓM, ΓK, and MK. The force constants needed for calculating the phonon dispersion are obtained by taking the derivatives of the potential as given by, for example, Maradudin *et al.*[17] The force constants depend on the choice of coordinate axes. The force constants between two atoms can also be written in terms of relative coordinates of the two atoms and the line joining the atoms by using the transformation given by Ref. 19. We represent the force-constant matrices in the crystallographic frame of reference with the X axis along the bond C1C2, as shown in Fig. 1. The origin of the coordinates is assumed to be at the lattice site occupied by the atom C1. The arrows in the figure denote the positive direction. The Z axis is assumed to be perpendicular to the graphene plane, which is the plane of the paper in Fig. 1.

A graphene unit cell contains two inequivalent atoms C1 and C2. We denote a lattice site by its two-dimensional (2D) position vector $\mathbf{l}$, where l_x and l_y are its x and y coordinates, respectively. The force-constant matrices $\boldsymbol{\phi}(0;\mathbf{l})$ between C1 and its first five nearest neighbors for different values of $\mathbf{l}$ are written in the following form appropriate for the hexagonal symmetry of graphene:

$$\boldsymbol{\phi}(0;2t,0) = -\begin{pmatrix} \alpha_1 & 0 & 0 \\ 0 & \beta_1 & 0 \\ 0 & 0 & \delta_1 \end{pmatrix}, \quad (28)$$

$$\boldsymbol{\phi}(0;0,2) = -\begin{pmatrix} \alpha_2 & \gamma_2 & 0 \\ -\gamma_2 & \beta_2 & 0 \\ 0 & 0 & \delta_2 \end{pmatrix}, \quad (29)$$

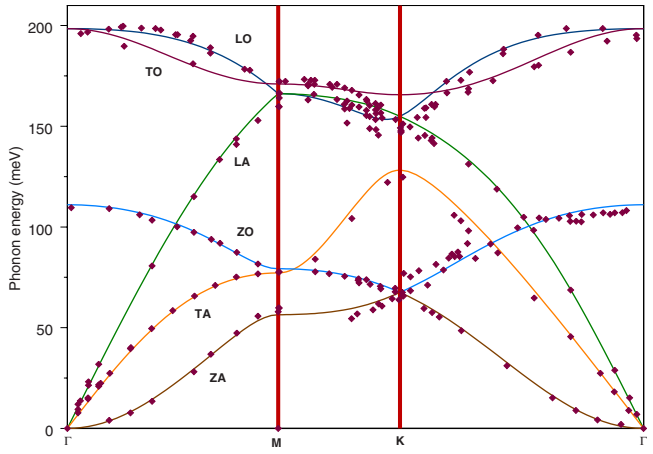

FIG. 2. (Color online) Phonon frequencies in energy units in the ΓM, MK, and ΓK directions as a function of the wave vector. Solid curves—calculated values. Dots—experimental values as quoted in Ref. 15 except for the ZO curve in the ΓK direction, which are taken from Ref. 20 and the ZA curve in MK direction, which are taken from Ref. 6.

$$\boldsymbol{\phi}(0;-4t,0) = -\begin{pmatrix} \alpha_3 & 0 & 0 \\ 0 & \beta_3 & 0 \\ 0 & 0 & \delta_3 \end{pmatrix}, \tag{30}$$

$$\boldsymbol{\phi}(0;5t,1) = -\begin{pmatrix} \alpha_4 & \gamma_4 & 0 \\ \gamma_4 & \beta_4 & 0 \\ 0 & 0 & \delta_4 \end{pmatrix}, \tag{31}$$

$$\boldsymbol{\phi}(0;6t,0) = -\begin{pmatrix} \alpha_5 & 0 & 0 \\ 0 & \beta_5 & 0 \\ 0 & 0 & \delta_5 \end{pmatrix}, \tag{32}$$

where $t=1/\sqrt{3}$. The form of the force-constant matrices between C1 and other atoms in the same neighbor shell and also between C2 and its neighbors can be similarly obtained from symmetry. Although our force constants are limited to fourth-neighbor interactions only, we have given the force-constant matrix for the fifth-neighbor atom at $(6t,0)$ in Eq. (32) for the sake of comparison with fifth-neighbor interaction models such as that by Mohr *et al.*[15] In our model $\alpha_5 = \beta_5 = \delta_5 = 0$.

From the force-constant matrices defined in Eqs. (28)–(31), we construct the dynamical matrix using the standard Fourier transform technique[17] and calculate the phonon frequencies. The force constants are calculated numerically by taking the appropriate derivates[17] of the total potential energy and are thus determined from the parameters of the interatomic potential. We choose these parameters such that a good fit is obtained between the calculated and the observed phonon frequencies in the three symmetry directions.

The calculated and the observed phonon frequencies are shown in Fig. 2 for the ΓM, ΓK, and MK directions of the wave vector. The experimental values have been taken from Mohr *et al.*[15] However, Mohr *et al.*[15] have not quoted the experimental values for the ZO curve in the ΓK direction and the ZA curve in the MK direction. In Fig. 2 therefore we have shown the experimental values obtained by Siebentritt *et al.*[20] for the ZO mode in the ΓK direction and those quoted by Wirtz and Rubio[6] for the ZA mode in the MK direction. The experimental values have been obtained by different techniques as described in the papers referred above. We see that the calculated phonon frequencies fit reasonably well with the observed frequencies considering that the interactions in our model are limited to fourth neighbors only. It would appear that the fifth-neighbor interactions have to be included to get a more perfect fit.[6,15]

The main features of our dispersion curves shown in Fig. 2 are similar to those obtained by the earlier authors,[6,15,21] who have given an excellent discussion of the nature of phonon dispersion in graphene. The most significant discrepancy between our results and those in Refs. 15 and 21 seems to be in the TA and ZO mode dispersion curves near the M point in the ΓM direction in Fig. 2. In our calculations they come close to each other at the M point. This is in contrast with the theoretical results of Zimmermann *et al.*[21] and Mohr *et al.*[15] that show that the two curves meet at the M point, which seems to be in agreement with the experimental results quoted by Mohr *et al.*[15] However, our results are consistent with the discussion given by Wirtz and Rubio.[6] There is of course no symmetry reason why the two curves must meet at M.

We calculate the elastic constants $c11$ and $c66$ in a dynamic rather than static sense by using the method of long waves.[17] This procedure automatically includes[17] the effect of internal lattice relaxation.[17,22] We compare the frequencies of the acoustic mode phonons polarized in the XY plane as predicted by the lattice-dynamical matrix in the long-wavelength limit with those predicted by the 2D Christoffel equations for elastic equilibrium. This amounts to assuming that the elastic constants $c11$ and $c66$ of graphene and graphite are equal. Physically, it means that the phonon frequencies of an elastic wave traveling in the XY plane in graphite depend only on the interactions between the atoms in that plane. This assumption can be justified because the interlayer interactions in graphite are much weaker than the intralayer interactions.

However, there is some obvious inconsistency in this procedure. The lattice-dynamical matrix is fully defined for a 2D solid because the Born von Karman equations depend on the mass of individual atoms and the location of discrete atomic sites in the 2D space. On the other hand, the Christoffel equations depend on the density of the solid, which is a three-dimensional (3D) parameter. Strictly speaking, 2D Christoffel equations correspond to plane strain in a 3D solid and not to a 2D solid, that is, a solid of zero thickness. In fact, the conventional elastic constants themselves are 3D parameters and are defined in a 3D volume.

Our procedure of calculating $c11$ and $c66$ for graphene, therefore, associates a volume with each atom in graphene. We assume that the volume per atom in graphene is equal to that in graphite. This assumption implies that the thickness of a graphene sheet is equal to the interlayer spacing in graphite. A similar assumption is also made about the thickness of carbon nanotubes in calculating their mechanical behavior.[1] This assumption is not strictly justified. However, since the

calculated values of the elastic constants depend strongly on the interatomic interactions, they serve to provide at least a qualitative estimate of the elastic stiffness of graphene. A more rigorous definition of the elastic constants for graphene would involve a precise quantum-mechanical calculation of the effective thickness of the graphene sheets.

We can of course define the elastic constants in a 2D space in units of force per unit length rather than force per unit area.[22,23] These 2D elastic constants can be obtained from our calculated values by multiplying them by the assumed thickness of the graphene layer, which, in our case as mentioned above, is equal to the interlayer spacing in graphite. We have verified that the result agrees with our static calculations of $c11$ and $c66$. We carried out the static calculations using the procedure given in an earlier paper.[24] However, measured values of 2D elastic constants are not yet available. Until such measurements are available, we suggest that $c11$ and $c66$ of graphite as calculated above can be regarded as a measure of the elastic stiffness of graphene. The agreement between the calculated values of $c11$ and $c66$ of graphene and their observed values for graphite, therefore, provides a qualitative validity of the fitted interatomic potential for graphene.

By comparing the frequencies predicted by the lattice-dynamical matrix in the long wavelength limit to those predicted by the Christoffel equations as described above, we obtain the following relations between the force constants and the elastic constants for graphene:

$$\begin{aligned} c11 = C_u[&2\alpha_1^2 + \alpha_1(6\alpha_2 + 19\alpha_3 + 35\alpha_4 + 54\alpha_5 + 6\beta_1 + 18\beta_2 + 3\beta_3 + 33\beta_4 + 18\beta_5 + 14\sqrt{3}\gamma_4) \\ &+ \alpha_2(6\alpha_3 + 12\alpha_4 + 6\beta_1 + 6\beta_3 + 12\beta_4) + 8\alpha_3^2 + \alpha_3(83\alpha_4 + 54\alpha_5 + 9\beta_1 + 18\beta_2 + 24\beta_3 + 21\beta_4 + 18\beta_5 + 2\sqrt{3}\gamma_4) \\ &+ 53\alpha_4^2 + \alpha_4(108\alpha_5 + 51\beta_1 + 36\beta_2 + 27\beta_3 + 162\beta_4 + 36\beta_5 + 40\sqrt{3}\gamma_4) + \alpha_5(54\beta_1 + 54\beta_3 + 108\beta_4) \\ &+ \beta_1(18\beta_2 + 9\beta_3 + 9\beta_4 + 18\beta_5 + 6\sqrt{3}\gamma_4) + \beta_2(18\beta_3 + 36\beta_4) + \beta_3(45\beta_4 + 18\beta_5 + 18\sqrt{3}\gamma_4) + 9\beta_4^2 + 36\beta_4\beta_5 - 12\gamma_4^2], \end{aligned} \tag{33}$$

$$\begin{aligned} c66 = C_u[&2\beta_1^2 + \beta_1(6\beta_2 + 19\beta_3 + 35\beta_4 + 54\beta_5 + 6\alpha_1 + 18\alpha_2 + 3\alpha_3 + 33\alpha_4 + 18\alpha_5 - 14\sqrt{3}\gamma_4) \\ &+ \beta_2(6\beta_3 + 12\beta_4 + 6\alpha_1 + 6\alpha_3 + 12\alpha_4) + 8\beta_3^2 + \beta_3(83\beta_4 + 54\beta_5 + 9\alpha_1 + 18\alpha_2 + 24\alpha_3 + 21\alpha_4 + 18\alpha_5 - 2\sqrt{3}\gamma_4) \\ &+ 53\beta_4^2 + \beta_4(108\beta_5 + 51\alpha_1 + 36\alpha_2 + 27\alpha_3 + 162\alpha_4 + 36\alpha_5 - 40\sqrt{3}\gamma_4) + \beta_5(54\alpha_1 + 54\alpha_3 + 108\alpha_4) \\ &+ \alpha_1(18\alpha_2 + 9\alpha_3 + 9\alpha_4 + 18\alpha_5 - 6\sqrt{3}\gamma_4) + \alpha_2(18\alpha_3 + 36\alpha_4) + \alpha_3(45\alpha_4 + 18\alpha_5 - 18\sqrt{3}\gamma_4) + 9\alpha_4^2 + 36\alpha_4\alpha_5 - 12\gamma_4^2], \end{aligned} \tag{34}$$

where

$$C_u = 1/[4c\sqrt{3}(\alpha_1 + \alpha_3 + 2\alpha_4 + \beta_1 + \beta_3 + 2\beta_4)], \tag{35}$$

and $c = 3.355$ Å is the interplanar separation in graphite. In deriving the above equations, we have used the fact that the volume per atom is equal to $a^2c\sqrt{3}$.

We have selected the parameters of our potential by fitting the values of $c11$ and $c66$, calculated as described above, with the observed values[25] for graphite. The calculated values of the two elastic constants are: $c11 = 1060$ and $c66 = 440$ GPa, which agree exactly with the experimental values given by Blakslee *et al.*[25] These values are slightly lower than $c11 = 1109$ and $c66 = 485$ GPa reported recently by Bosak *et al.*[26] We could have fitted our parameters with the values given by Bosak *et al.*[26] but we chose the values reported by Blakslee *et al.*[25] partly because they have been widely used in the literature and also because they are most consistent with Brillouin-light-scattering measurements on highly oriented pyrolytic graphite recently performed in our laboratory in Ref. 27.

The final list of all the parameters of the potential function in Eq. (1) is given below. Parameters for the bond energy function are as follows:

$$\alpha a = 3.31, \quad \beta a = 4.038, \quad R_0 = 2/\sqrt{3},$$

$$A = -156.242 \text{ eV}, \quad B = -1187.6 \text{ eV},$$

$$\mu_1 = -0.3064, \quad \mu_2 = 0.2597, \quad \gamma a = -0.3256,$$

$$\lambda_1 = -0.1022, \quad \lambda_2 = 0.09724$$

Coefficients in the radial energy function (in eV) are as follows:

$$Q_1 = -7.0436 \times 10^{-3}, \quad Q_2 = -19.3375,$$

$$Q_3 = -28.542, \quad Q_4 = 0.3669,$$

$$S_1 = -0.08481, \quad S_2 = -257.027,$$

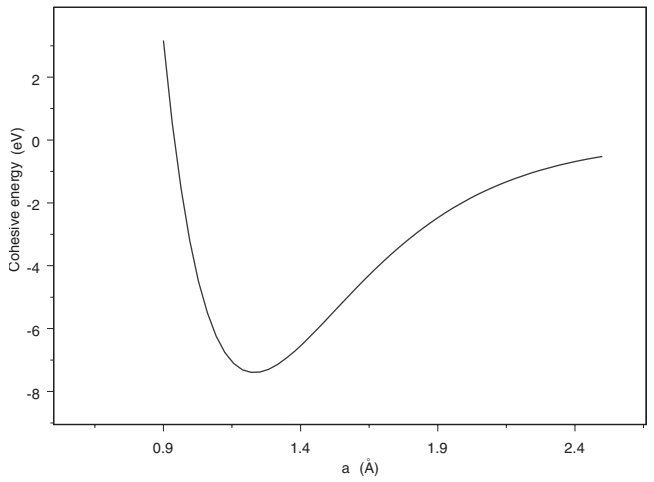

FIG. 3. Cohesive energy (eV) per atom in an undeformed graphene lattice as a function of a, half the lattice constant (Å).

$$S_3 = 124.909, \quad S_4 = -1.4570.$$

Nodes in the radial energy function (up to fourth-nearest-neighbor distances) are as follows:

$$R_1 = 2/\sqrt{3}, \quad R_2 = 2, \quad R_3 = 4/\sqrt{3}, \quad R_4 = 2\sqrt{(7/3)}.$$

We calculate the total cohesive energy of the undeformed graphene lattice by using Eq. (1) and the parameters as given above. In an undeformed graphene lattice all the atoms are located at the hexagonal lattice sites. The contribution of the radial potential energy in this case is zero. The total cohesive energy per atom as a function of a, half the lattice constant, is shown in Fig. 3. As expected the minimum is at $a = 1.231$ Å and the energy at the minimum is −7.40 eV.

We calculate the force constants by taking the derivatives of the total potential energy at the lattice sites in the perfect graphene lattice.[17] The calculated values of the force constants as defined in Eqs. (28)–(32) are given below in N/m,

$$\alpha_1 = 409.705, \quad \beta_1 = 145.012, \quad \delta_1 = 98.920,$$

$$\alpha_2 = -40.8, \quad \beta_2 = 74.223, \quad \gamma_2 = -9.11, \quad \delta_2 = -8.191,$$

$$\alpha_3 = -33.203, \quad \beta_3 = 50.10, \quad \delta_3 = 5.802,$$

$$\alpha_4 = 10.539, \quad \beta_4 = 4.993, \quad \gamma_4 = 2.184, \quad \delta_4 = -5.213,$$

$$\alpha_5 = \beta_5 = \delta_5 = 0.$$

Finally, we calculate the flexural rigidity of graphene using our force constants. An important characteristic of the phonon-dispersion curves for graphene is that the phonon frequency of the ZA mode is a quadratic function of the wave vector in the long-wavelength limit.[15,18,19] The coefficient of the linear term in the dispersion relation is zero. The coefficient of the quadratic term gives the flexural rigidity of graphene. Following the method given in Ref. 18, we obtain the following expression for the flexural rigidity of graphene for the present model:

$$D = -(\sqrt{3}/36)(\delta_1 + 18\delta_2 + 16\delta_3 + 98\delta_4 + 162\delta_5)a^2. \tag{36}$$

Using the values of the force constants given above and $a = 1.231$ Å, we obtain $D = 2.13$ eV. This value is much larger than the value 0.797 eV calculated earlier[18] using the TB model potential. The difference between the two is not surprising because the third and fourth-neighbor force constants make a significant contribution, as is apparent from Eq. (36). These force constants have been neglected in the TB model.

IV. CONCLUSIONS

We have proposed a functional form for the interatomic potential in graphene. The potential energy is expressed in two parts—the bond energy part and the radial energy part. As in the TB model, the bond energy part is represented as a combination of two exponentials with their coefficients depending on the environment. Unlike the TB model, the coefficients of the exponentials are represented by functions that explicitly account for distortions normal to the plane of graphene. These functions should therefore be more reliable for modeling ripples, which are very important for the stability of graphene.[16] The radial part of the potential energy is represented in terms of polynomials that extend up to fourth-neighbor distance from an atom and has nodes or zeros at the undeformed lattice sites. The radial part does not contribute to the cohesive energy of the perfect graphene lattice at equilibrium. It contributes only to the interatomic force constants.

The total potential has 13 adjustable parameters that are determined by fitting the calculated and observed values of the cohesive energy, lattice constant, elastic constants $c11$ and $c66$, and the phonon frequencies in the three symmetry directions ΓM, ΓK, and MK. The overall fit between all the calculated and experimental values is found to be very good.

Our model potential is broadly based on the TB model. The form of the angular functions in our model is different and we have also added a separate radial term. The TB model is more general than our model and is applicable to different clusters of carbon atoms where our potential is meant specifically for graphene and clusters of atoms around the graphene lattice sites. The equilibrium lattice structure of graphene is built into our model potential. Like the TB model, our potential is expressed in terms of analytical functions, which makes it convenient for computer simulations. Both the models give a very good fit between the calculated and the observed values of the cohesive energy and the lattice constant of graphene.

However, the TB model does not give the correct elastic constants and the phonon frequencies for graphene or graphite. The main advantage of our potential over the TB model for application to graphene is that our potential yields a very good agreement between the calculated and the observed values of the elastic constants and the phonon frequencies over the entire Brillouin zone of graphene. This is achieved because the range of the interaction of an atom in our model extends up to its fourth-nearest neighbors in contrast to the TB model in which the range of interaction is limited to only

second-neighbor distance. It is necessary to include[6] at least up to fourth-neighbor interactions for obtaining a good fit with the observed phonon frequencies. In order to improve the fit for the phonon frequencies, the fifth-neighbor interactions need to be included as has been shown recently by Mohr *et al.*[15]

We have given the values of the interatomic force constants for up to fourth-nearest neighbors of each atom. These parameters should be useful for lattice statics and lattice dynamics calculations. In the harmonic approximation, lattice statics and lattice dynamics calculations depend only on the force constants and not on the detailed form of the potential. However, in many cases of current physical interests as in nanomaterials, it is necessary to include some anharmonic effects. These calculations may not be sensitive to the detailed structure of the potential and it may be enough to know the variation in the potential near the lattice sites. Our model potential should be particularly useful for such calculations.

Very interesting work on the force constants and phonon dispersion in graphene have been published by Saito *et al.*,[19] Wirth and Rubio,[6] Mohr *et al.*,[15] and Zimmermann *et al.*[21] They have, however, not given the interatomic potential whereas our main interest is in the interatomic potential. The interatomic potential is needed, for example, for molecular dynamics and other computer simulations of the solid. Our results for the force constants and the phonon frequencies are generally similar to them with some differences in the quality of fitting. Zimmermann *et al.*[21] have not given a comparison of their calculated phonon frequencies with the experimental values but we find that they qualitatively agree with the experimental results.

An important qualitative difference between the different force-constant models quoted above is in the off-diagonal element γ_2 in the second-neighbor force-constant matrix $\phi(0;0,2)$ given in Eq. (29). It has been assumed to be zero in the models of Saito *et al.*,[19] Mohr *et al.*,[15] and Zimmermann *et al.*[21] but not in our model and in that of Wirtz and Rubio.[6] There is no symmetry reason for this term to be zero. The contribution of this term can be quite significant as it affects the crossing of the LO-TO curve in the ΓM direction.[6]

Another important difference between our model and the force-constant models quoted above is in the predicted values of the elastic constants. The values of the elastic constants have not been reported by the authors of the force-constant models quoted above. For the sake of comparison, we have calculated $c11$ and $c66$ for those force-constant models using the long-wave limit procedure described in Sec. III. We find that $c11$ and $c66$, respectively, are, in units of gigapascal, 846 and 248 for the TB potential, 1011 and 509 for the model of Saito *et al.*,[19] 990 and 443 for the model of Wirtz and Rubio,[6] 1208 and 466 for the model of Mohr *et al.*,[15] and 919 and 255 for the model of Zimmermann *et al.*[21] All the above values differ significantly with the observed values for graphite[25] $c11=1060$ and $c66=440$ GPa. The values given by our model are $c11=1060$ and $c66=440$ GPa, which fit exactly with the observed values for graphite.

The discrepancy in the predicted and the observed values of $c11$ and $c66$ does not necessarily reflect on the lack of validity of these models for the purpose of interpreting the phonon frequency data. Presumably, the objective of the authors was to model the phonon frequencies over the entire zone and they did not try to fit the force constants with the elastic constants of graphite. However, in absence of the measured values of the elastic constants of graphene, we feel that, for calculations of the mechanical properties of graphene, it is better to use a potential and a set of force constants that yield the correct values of the $c11$ and $c66$ of graphite. Our potential function as given in Eq. (1) should serve this need.

Finally, we have also calculated the flexural rigidity of graphene using a formula derived earlier[18] by using Green's-function method. We obtain the value of the flexural rigidity to be 2.13 eV. This value is much larger than 0.797 eV calculated earlier by using the second-neighbor TB model. This is not surprising because the third and fourth neighbors make a substantial contribution to the flexural rigidity. Since the present model gives a better agreement with the observed phonon frequencies, the present value of 2.13 eV should be more reliable than the previously calculated value.

ACKNOWLEDGMENTS

The authors thank W. J. Johnson and Ke-Gang Wang for reading the paper and their useful comments.

*FAX: 303-497-5030; tewary@boulder.nist.gov

[1] D. Qian, G. J. Wagner, W. K. Liu, M. F. Yu, and R. S. Ruoff, Appl. Mech. Rev. **55**, 495 (2002).
[2] B. I. Dunlap and J. C. Boettger, J. Phys. B **29**, 4907 (1996).
[3] G. T. Gao, K. Van Workum, J. D. Schall, and J. A. Harrison, J. Phys.: Condens. Matter **18**, S1737 (2006).
[4] M. U. Kahaly and U. V. Waghmare, J. Nanosci. Nanotechnol. **7**, 1787 (2007).
[5] N. Mounet and N. Marzari, Phys. Rev. B **71**, 205214 (2005).
[6] L. Wirtz and A. Rubio, Solid State Commun. **131**, 141 (2004).
[7] H. Yanagisawa, T. Tanaka, Y. Ishida, M. Matsue, E. Rokuta, S. Otani, and C. Oshima, Surf. Interface Anal. **37**, 133 (2005).
[8] D. W. Brenner, Phys. Rev. B **42**, 9458 (1990).
[9] M. Dagher, M. Kobersi, and H. Kobeissi, J. Comput. Chem. **16**, 723 (1995).
[10] A. Liu and S. J. Stuart, J. Comput. Chem. **29**, 601 (2008).
[11] J. Tersoff, Phys. Rev. Lett. **61**, 2879 (1988).
[12] M. I. Baskes, Phys. Rev. Lett. **59**, 2666 (1987).
[13] F. H. Stillinger and T. A. Weber, Phys. Rev. B **31**, 5262 (1985).
[14] J. H. Los, L. M. Ghiringhelli, E. J. Meijer, and A. Fasolino, Phys. Rev. B **72**, 214102 (2005).
[15] M. Mohr, J. Maultzsch, E. Dobardzic, S. Reich, I. Milosevic, M. Damnjanovic, A. Bosak, M. Krisch, and C. Thomsen, Phys. Rev. B **76**, 035439 (2007).

[16] A. Fasolino, J. H. Los, and M. I. Katsnelson, Nat. Mater. **6**, 858 (2007).
[17] A. A. Maradudin, E. W. Montroll, G. H. Weiss, and I. P. Ipatova, *Theory of Lattice Dynamics in the Harmonic Approximation* (Academic, New York, 1971).
[18] B. Yang and V. K. Tewary, Phys. Rev. B **77**, 245442 (2008).
[19] R. Saito, G. Dresselhaus, and M. S. Dresselhaus, *Physical Properties of Carbon Nanotubes* (Imperial College, London, 2004).
[20] S. Siebentritt, R. Pues, K. H. Rieder, and A. M. Shikin, Phys. Rev. B **55**, 7927 (1997).
[21] J. Zimmermann, P. Pavone, and G. Cuniberti, Phys. Rev. B **78**, 045410 (2008).
[22] J. Zhou and R. Huang, J. Mech. Phys. Solids **56**, 1609 (2008).
[23] M. Arroyo and T. Belytschko, Phys. Rev. B **69**, 115415 (2004).
[24] B. Yang and V. K. Tewary, Phys. Rev. B **75**, 144103 (2007).
[25] O. L. Blakslee, D. G. Proctor, E. J. Seldin, G. B. Spence, and T. Weng, J. Appl. Phys. **41**, 3373 (1970).
[26] A. Bosak, M. Krisch, M. Mohr, J. Maultzsch, and C. Thomsen, Phys. Rev. B **75**, 153408 (2007).
[27] W. L. Johnson and S. A. Kim (private communication).